

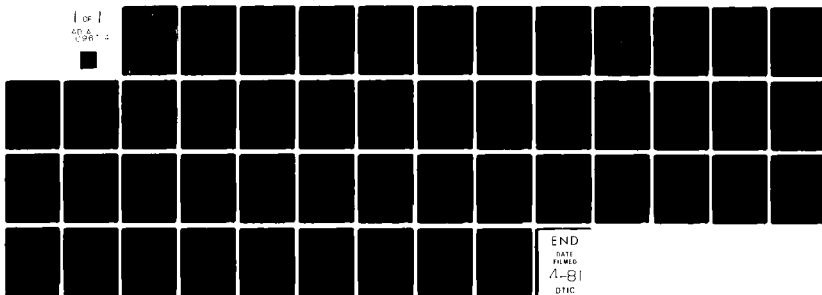
AD-A096 714 GENERAL ELECTRIC CO SYRACUSE NY MILITARY ELECTRONIC --ETC F/6 17/1
THE OPTICAL GRATING HYDROPHONE.(U)

JAN 81 B W TIETJEN

UNCLASSIFIED R01EMH1

NL

(of)
AD-A096 714



END
DATE
FILMED
A-81
DTIC

TIS Distribution Center
CSP 4-18, X7712
Syracuse, New York 13221

— LEVEL II

5

B.S.

GENERAL ELECTRIC

MILITARY ELECTRONIC SYSTEMS OPERATION

9 TECHNICAL INFORMATION SERIES

Author B. W. Tietjen	Subject Category Hydrophone Development	No. R81EMH1
Title THE OPTICAL GRATING HYDROPHONE		Date Jan 81
Copies Available at MESO TIS Distribution Center Box 4840 (CSP 4-18) Syracuse, New York 13221	GE Class 1 Govt Class Unclassified	No. of Pages 47
<p>Summary</p> <p>An optical hydrophone has been developed, the output of which is a direct intensity modulated representation of an incident acoustic field. The principle of operation involves the relative displacement induced by an acoustic field of two optical gratings which lie between a constant optical source and an optical receiver. The received light intensity is a function of the relative displacement of the two optical gratings.</p> <p>The optical source may be coherent or incoherent light, and a simple pin photodiode detector affords adequate receiver sensitivity. Large, multimode optical fibers can be used to carry the light to and from the hydrophone, and since the device is photon-noise limited, arbitrarily high sensitivities can be obtained by increasing the optical power.</p> <p>The direct intensity modulated output eliminates the need for more sophisticated detection techniques that are often applied to phase modulating optical hydrophones, yet comparable sensitivity can be realized with the optical grating approach.</p> <p>Fabrication of the device is straightforward, without any advanced optical techniques required. Several prototypes have been built and have already demonstrated dynamic ranges as high as 160 dB, with the ability to detect acoustically induced displacements of less than 0.01 Angstroms.</p>		

12 49
DTIC ELECTE
MAR 24 1981

E

This document contains proprietary information of the General Electric Company and is restricted to distribution and use within the General Electric Company unless designated above as GE Class 1 or unless otherwise expressly authorized in writing.

DTIC FILE COPY

81 3 20 039

Send to

411962

GENERAL ELECTRIC COMPANY TECHNICAL INFORMATION

Within the limitations imposed by Government data export regulations and security classifications, the availability of General Electric Company technical information is regulated by the following classifications in order to safeguard proprietary information:

CLASS 1: GENERAL INFORMATION

Available to anyone on request.
Patent, legal and commercial review
required before issue.

CLASS 2: GENERAL COMPANY INFORMATION

Available to any General Electric Company
employee on request.
Available to any General Electric Subsidiary
or Licensee subject to existing agreements.
Disclosure outside General Electric Company
requires approval of originating component.

CLASS 3: LIMITED AVAILABILITY INFORMATION

Original Distribution to those individuals with
specific need for information.
Subsequent Company availability requires
originating component approval.
Disclosure outside General Electric Company
requires approval of originating component.

CLASS 4: HIGHLY RESTRICTED DISTRIBUTION

Original distribution to those individuals personally responsible for the Company's interests in the subject.
Copies serially numbered, assigned and recorded by name.
Material content, and knowledge of existence, restricted to copy holder.

GOVERNMENT SECURITY CLASSIFICATIONS, when required, take precedence in the handling of the material. Wherever not specifically disallowed, the General Electric classifications should also be included in order to obtain proper handling routines.

GENERAL ELECTRIC COMPANY
MILITARY ELECTRONIC SYSTEMS OPERATIONS
TECHNICAL INFORMATION SERIES

SECTION UEPD
UNIT Sonar Information Proc Sys
MESO ACCOUNTING REFERENCE 339
COLLABORATORS _____
APPROVED M.B. McGuinness TITLE Mgr Sonar LOCATION FRP 1-N1
M. B. McGuinness Sig Proc

MINIMUM DISTRIBUTION - Government Unclassified Material (and Title Pages) in G.E. Classes 1, 2, or 3 will be the following.

<u>Copies</u>	<u>Title Page Only</u>	<u>To</u>
0	1	Legal Section, MESO (Syracuse)
0	1	Manager, Technological Planning, MESO (Syracuse)
5	6	G-E Technical Data Center (Schenectady)

MINIMUM DISTRIBUTION - Government Classified Material, Secret or Confidential in G.E. Classes 1, 2, or 3 will be the following.

1	0	Manager, Technological Planning, MESO (Syracuse)
---	---	--

ADDITIONAL DISTRIBUTION (Keep at minimum within intent of assigned G.E. Class.)

<u>COPIES</u>	<u>NAME</u>	<u>LOCATION</u>
5 (CLASS 1 ONLY)	DEFENSE DOCUMENTATION CENTER	CAMERON STATION, ALEXANDRIA, VA. 22314
1	L.I. Chasen	P.O. Box 8555 Philadelphia, Pa., 19101
2	B.W. Tietjen	FRP 1 IN, Syracuse, NY 13221
1	M.B. McGuinness	FRP 1 IN, Syracuse, NY 13221
1	L. Knickerbocker	FRP 1 IN, Syracuse, NY 13221
1	S. Garber	CSP 4-48, Syracuse, NY 13221
1	Dr. R.J. Talham	FRP 1-5A, Syracuse, NY 13221
1	Dr. D. Gilbert	CSP 4-49, Syracuse, NY 13221
1	Dr. E. Monsay	CSP 4-48, Syracuse, NY 13221
1	J. Jackson	FRP 1-4J, Syracuse, NY 13221
1	J. Chovan	EP 2-216, Syracuse, NY 13221
1	Dr. M. Fitelson	EP 3-318, Syracuse, NY 13221
1	E. Ferris	EP 3-218, Syracuse, NY 13221
1	E. Valovage	CSP4-56, Syracuse, NY 13221

ACKNOWLEDGEMENTS

The author wishes to thank Joseph Chovan for the Homodyne Noise Analysis Section, and in general for providing insight into the theoretical operation and sensitivities of the optical grating hydrophone.

Also to Edward Valovage who performed the optical noise measurements to verify theoretical predictions.

Accession For	
NTIS GRA&I	<input checked="checked" type="checkbox"/>
ERIC TAB	<input type="checkbox"/>
Unannounced	<input type="checkbox"/>
Justification	
By	
Distribution/	
Availability Codes	
Full and/or	
Dist	Special
A	

GLOSSARY

A	--	Amperes
Å	--	Angstrom
C	--	Coulombs
dB	--	Decibel
dc	--	Direct Current
F	--	Fahrenheit
gcm	--	Gram centimeters
Hz	--	Hertz
J	--	Joules
K	--	Kelvin
kHz	--	Kilohertz
m	--	Meter
MDS	--	Minimum Detectable Signal
mm	--	Millimeter
mW	--	Milliwatts
NEP	--	Noise Equivalent Power
nm	--	Nanometer
OGH	--	Optical Grating Hydrophone
rms	--	Root-Mean-Square
s	--	Seconds
SNR	--	Signal-to-Noise Ratio
V	--	Volts
W	--	Watts
μbar	--	Microbars
μW	--	Microwatts
Ω	--	Ohms

TABLE OF CONTENTS

<u>Section</u>	<u>Title</u>	<u>Page</u>
I	INTRODUCTION	1-1
	1.1 Background	1-1
II	RESULTS AND CONCLUSIONS	2-1
	2.1 Self-Noise	2-1
	2.2 Hydrophone Sensitivity and Dynamic Range	2-3
III	CONCLUSIONS AND DISCUSSION ON THE OPTICAL GRATING HYDROPHONE	3-1
IV	ANALYSIS	4-1
	4.1 Theoretical Introduction	4-1
	4.2 Performance Analysis	4-6
	4.2.1 System Noise	4-6
	4.2.2 Electronic Noise	4-6
	4.2.3 Resistor Thermal Noise	4-7
	4.2.4 Photon Noise	4-7
	4.2.5 Homodyning Noise	4-9
	4.2.6 Conclusion on Optical Noise	4-14
	4.3 Sensitivity/Dynamic Range Analysis	4-14
	4.3.1. General	4-14
	4.3.2 Minimum Bias (α)	4-18
V	REFERENCES	5-1/5-2
APPENDIX A	OPTICAL NOISE MEASUREMENTS	A-1
	1. Introduction	A-1
	2. Procedure	A-1
	3. Conclusions	A-5

LIST OF ILLUSTRATIONS

<u>Figure</u>	<u>Title</u>	<u>Page</u>
1-1	Movable Grating Optical Hydrophone Principle	1-2
2-1	SNR vs Detector Output Voltage	2-2
2-2	Dynamic Range vs P_{IN} for Various α for Photon Photon Noise-Limited System	2-4
2-4	Optical Grating Hydrophone MDS Levels Superimposed on Background Sea Noise Curves	2-8
2-3	Optical Grating Hydrophone MDS Levels Superimposed on Background Sea Noise Curves	2-7
4-1	Rectangular Grating (Dimension HW) Uniformly Illuminated by Total Intensity Optical Source	4-4
4-2	Optical Power Spectrum	4-10
4-3	MDS Level vs Frequency for $\alpha = \alpha_m$	4-21
A-1	The Optical Noise Measurement Test Setup	A-2
A-2	Experimental and Calculated Data	A-6

SECTION I

INTRODUCTION

The Optical Grating Hydrophone (OGH) is a device which converts a time-varying acoustic field to an intensity-modulated optical field. The optical intensity is linearly related to the incident acoustic field.

The hydrophone itself consists basically of two optical waveguides (or fibers) in axial alignment with a slight gap between them. An aperture of controlled optical transmittance in the gap provides the desired intensity modulation.

The controllable aperture is comprised of two identical bar gratings having opaque and transparent parallel stripes of equal width. The gratings are overlaid and slide with respect to each other to control the net transparent area. Hence the two gratings act like a shutter which is controlled by the acoustic field in some fashion, as shown in Figure 1-1.

When the opaque stripes of one grating coincide with the transparent stripes of the other grating, the net transparent area (transmittance) is zero. As the gratings are translated with respect to each other so that the transparent stripes of one coincide with the transparent stripes of the other, the net transparent area is one-half of the total area. The optical transmission from one optical waveguide to the other, therefore, varies linearly from zero to essentially one-half the waveguide area, neglecting the slight loss associated with the beam divergence across the gap.

The spacial frequency and static setting of the gratings, together with the optical power used, determine the sensitivity and dynamic ranges of the optical grating hydrophone.

This report presents some background, theory of operation, and sensitivity/dynamic range analyses of the OGH.

1.1 BACKGROUND

The recent advances in fiber optic technology has stimulated interest in applying fiber optics to sonar systems. Optical fibers offer lighter weight, smaller size, and higher immunity to electromagnetic interference than conventional wiring. Size and weight reductions are substantial when conventional wiring is replaced with optical drivers, fibers, and receivers.

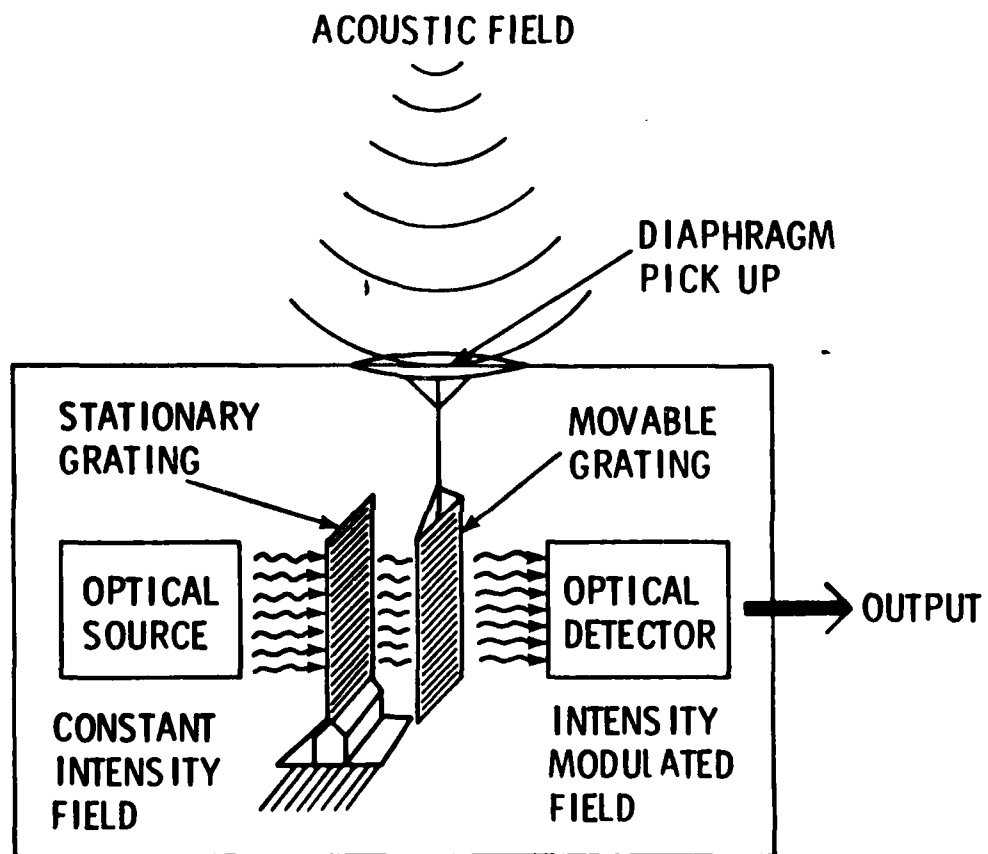


Figure 1-1. Movable Grating Optical Hydrophone Principle

In conjunction with the interest in optical fibers for sonar systems, is a drive to develop an optical hydrophone in which the acoustic information is superimposed on an optical carrier. The optical information can be carried by optical fibers, and could significantly reduce or even eliminate the electronics external to a given vehicle. This would reduce the weight and even increase the reliability of external hydrophone arrays. Other advantages of optical hydrophones are discussed by Bucaro [1] .

Several types of optical hydrophones are currently under development [2] . These can be categorized into two basic types - coherent and incoherent.

Coherent optical hydrophones typically require coherent sources (lasers), very small (single mode) optical fibers, and some type of interferometric or phase detection schemes to extract the acoustic information, which is in the form of optical phase or frequency modulation. More detailed accounts of the various coherent optical hydrophones can be found in References [1, 3, 4 and 5] .

Incoherent optical hydrophones on the other hand, do not require lasers, can use large fibers, and their output is an intensity modulated optical signal, so only a simple photodetector is necessary to extract acoustic information from the received light. From these characteristics, the incoherent, intensity modulating types of optical hydrophones would appear more desirable from a sonar systems point-of-view with present state-of-the-art technology [6, 7] .

Several incoherent optical hydrophone (and/or microphone) techniques have been considered and are listed below:

1. Specular Reflection [8, 9]
2. Frustrated Internal Reflection [8]
3. Bending Loss in Optical Fibers [2]
4. Evanescent Wave Coupling Phenomenon [2]
5. Polarization Techniques
6. Relative Displacement of Optical Waveguides
7. Oscillating Mirror [10]
8. Optical Grating Technique (Relative Displacement of Optical Gratings) [7, 11]

Of these techniques, the optical grating approach appears to be among the most feasible in the near term. It promises to offer the sensitivities and dynamic ranges expected of a practical optical hydrophone [7] .

SECTION II

RESULTS AND CONCLUSIONS

2.1 SELF-NOISE

Analysis and test results show that there are two main sources of noise for practical light levels. These are photon noise and thermal noise of the bias resistor in the detector circuit. The signal-to-noise ratio (SNR) can be defined as the ratio of the average voltage resulting from the incident average optical power, to the noise voltage associated with thermal and photon noise. The expression for this SNR is given as:

$$\text{SNR} = \frac{V^2}{(2eVR + V_R^2) B} \quad (2-1)$$

where

- V = Average voltage across R due to optical bias power
- V_R = Voltage due to thermal noise of R
- R = Detector resistor value
- e = Electronic charge (1.6×10^{-19} C)
- B = Bandwidth of measurement

Since

$$V^2 = 4KTBR, \text{ write:}$$

$$\text{SNR} = \frac{V^2}{2RB (eV + 2kT)} \quad (2-2)$$

where

- T = Temperature of resistor in °K ($70^\circ\text{F} = 294^\circ\text{K}$)
- K = Boltzmann's constant (1.38×10^{-23} J/°K)

The SNR value is plotted versus average level V in Figure 2-1 for a resistor value of 33,200 Ω.

Note that as optical levels increase (increased V) the system becomes photon noise limited (i.e., $V_R^2 \ll 2eVR$) and the SNR expression reduces to:

$$\text{SNR}_p = \frac{V}{2eRB} \quad (2-3)$$

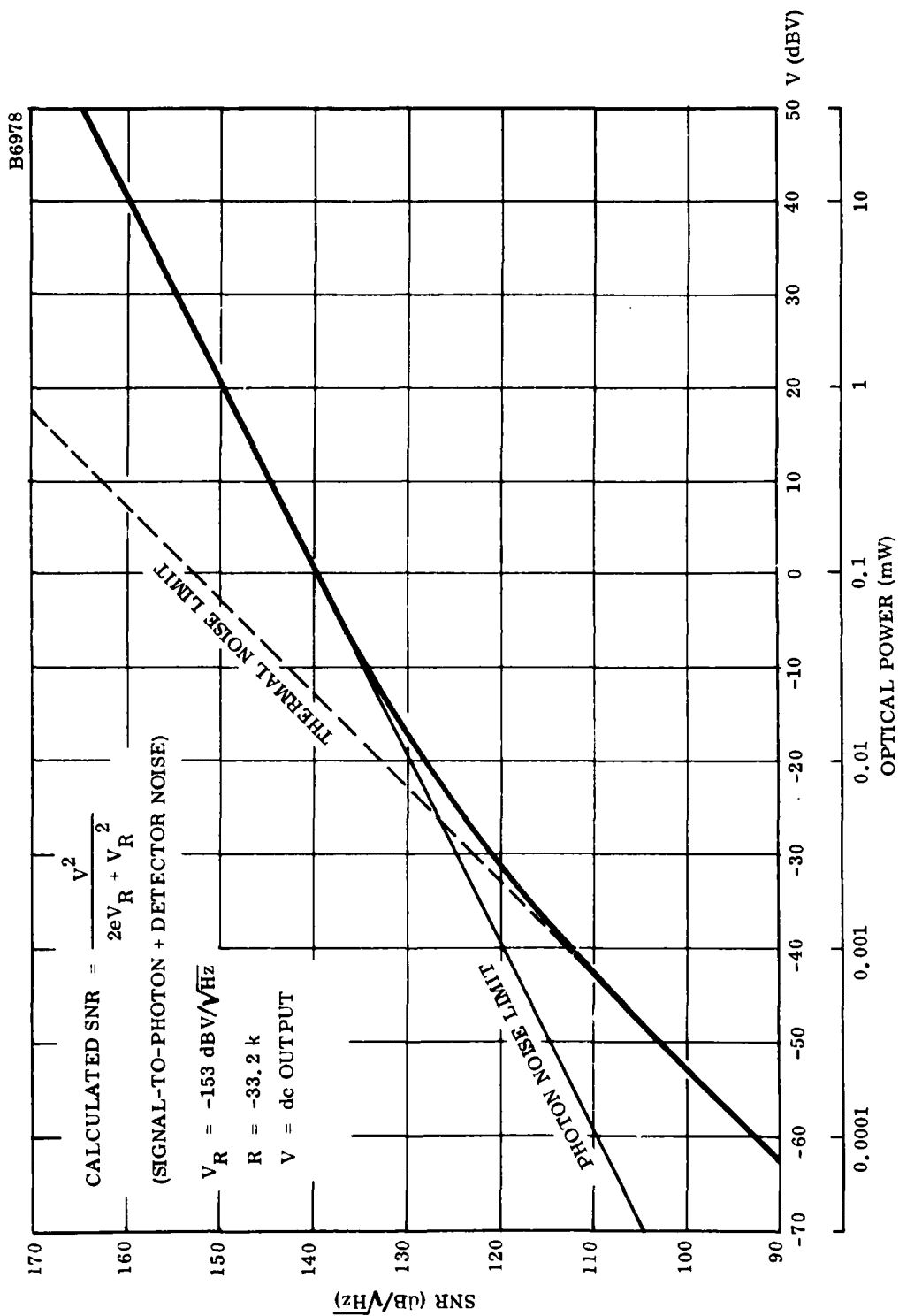


Figure 2-1. SNR vs Detector Output Voltage

V/R can be related to incident optical power by:

$$\frac{V}{R} = \frac{P_o \eta e}{h \nu} = i \quad (2-4)$$

where:

- P_o = Total optical power incident upon the photodetector
- h = Plank's constant (6.63×10^{-34} J-s)
- i = Current due to optical power
- η = Quantum efficiency (typically about 0.5)
- ν = Optical frequency (4.5×10^{14} Hz)

The signal-to-photon noise ratio written in terms of incident optical power, P_o , therefore, is, for a photon noise limited system:

$$SNR_p = \frac{P_o \eta}{2h \nu B} \quad (2-5)$$

Figure 2-1 shows that photon noise becomes the limiting factor for voltages above -10 dBV, which corresponds to optical powers of 0.036 mW and above. Typically, several milliwatts of optical power can be easily used, so photon noise will indeed be the limiting factor in a practical system. This implies that arbitrarily high sensitivities and dynamic range (high SNR_p) can be obtained by using more optical power.

2.2 HYDROPHONE SENSITIVITY AND DYNAMIC RANGE

The dynamic range is defined here as the ratio of maximum undistorted signal-to-photon noise levels, and is expressed as:

$$DR = \frac{P_{IN} \eta \alpha}{8h \nu B} \quad (2-6)$$

where P_{IN} is the total optical power incident upon the gratings, and α is proportional to the static, or average, optical power transmitted through the gratings. When $\alpha = 0$, no light is transmitted, and when $\alpha = 1$, half of the light incident upon the gratings is transmitted. The quantity α is therefore a measure of the bias of the system. Equation (2-6) is plotted for various P_{IN} and α in Figure 2-2 (for $\eta = 0.5$).

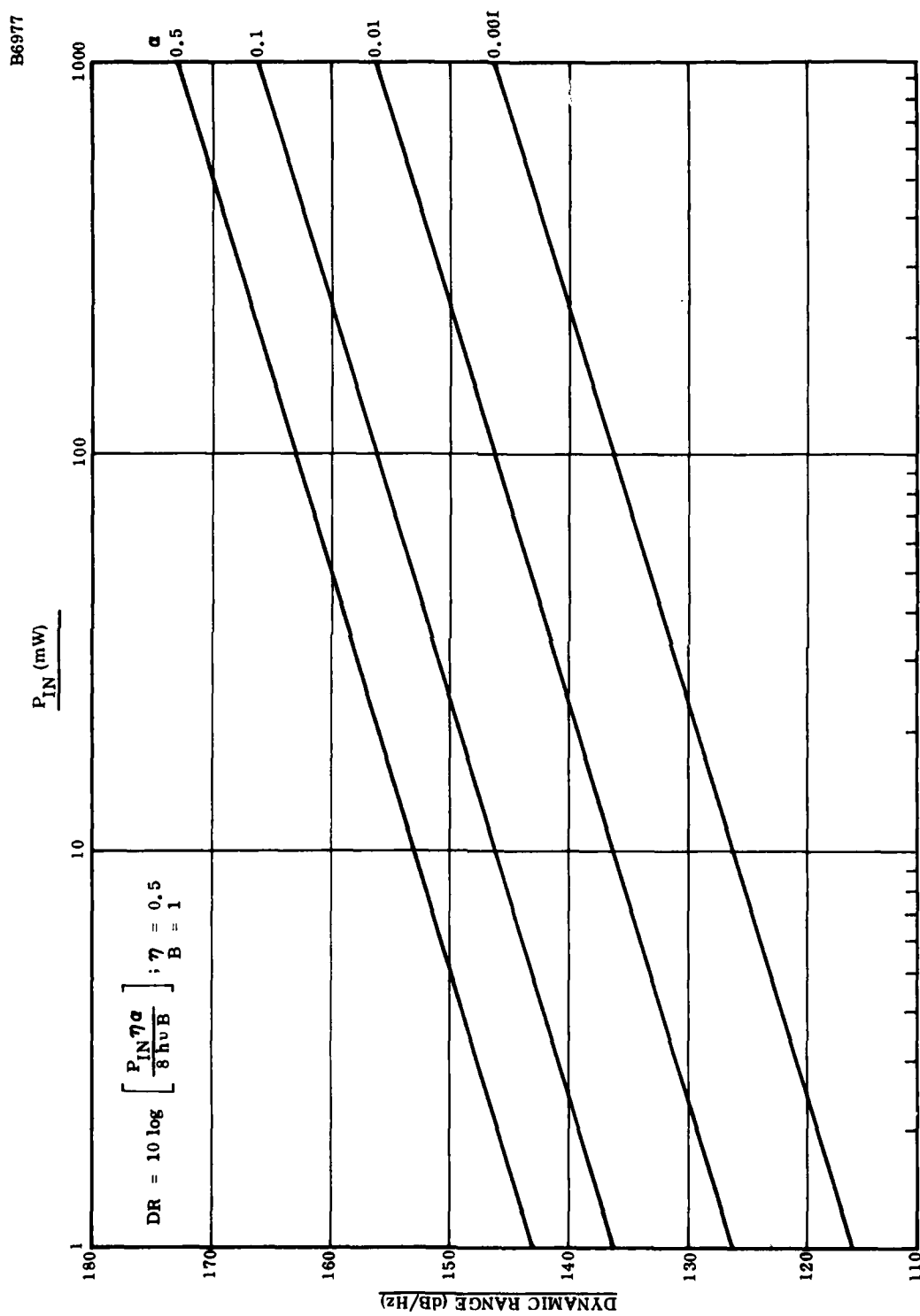


Figure 2-2. Dynamic Range vs P_{IN} for Various α for Photon Noise-Limited System

The minimum rms displacement of the gratings, δ_M , that will yield a 0 dB signal-to-photon noise ratio is given by:

$$\delta_M^2 = \frac{4h\nu B\alpha L^2}{P_{IN}\eta} \quad (2-7)$$

where:

L = Distance between grating lines (i.e., one half of the spatial period of the gratings)

If, in order to proceed with our analysis, we assume that the grating displacement equals the particle motion of the water due to an incident acoustic signal, then the maximum achievable sensitivity can be determined.

Note that for a specific hydrophone design one may evaluate performance in terms of grating-motion as a fraction of particle-motion and, hence, derive a multiplying factor for that design which describes how it approaches the maximum achievable sensitivity.

The hydrophone sensitivity is the minimum sound pressure level that results in a 0 dB signal-to-photon noise ratio at the hydrophone output, and is written as:

$$P^2 = \frac{4h\nu(\omega\rho cL)^2\alpha B}{P_{IN}\eta} \quad (2-8)$$

or, in terms of the spatial frequency, D , of the gratings and letting $\omega = 2\pi f$, the minimum detectable signal (MDS) level becomes:

$$P^2 = \frac{Bh\nu(2\pi\rho c)^2}{\eta} \frac{f^2\alpha}{P_{IN}D^2} \quad (2-9)$$

where:

ρc = Specific acoustic impedance of sea water ($1.55 \times 10^5 \text{ gcm}^{-2} \text{ s}^{-1}$)

f = Acoustic frequency

D = Spatial frequency of gratings

For D in units of lines per inch (D_{IN}), and P_{IN} in units of milliwatts, the MDS level can be expressed as:

$$\frac{P^2}{B} = (3.651 \times 10^{-6}) \frac{f^2\alpha}{P_{IN}D_{IN}^2} \mu\text{bar}^2/\text{Hz} \quad (2-10)$$

Equation (2-10) implies that the hydrophone sensitivity can be increased (MDS level decreased) by:

- Increasing Grating Density, D_{IN}
- Increasing Optical Power, P_{IN}
- Decreasing the Bias, α .

Figure 2-3 is a plot of P^2/B superimposed on existing sea-state curves. Here, the input power is fixed at 100 mW, the bias α , at 0.5, and the grating densities varied from 100 to 10,000 lines per inch. These curves show that the optical grating hydrophone, for the given parameters is adequate to detect low sea states and shipping noises at frequencies below 1 kHz.

Figure 2-4 is similar to Figure 2-3 except that the input power has been increased to 1W, and the bias decreased to 0.01 in an attempt to increase the sensitivity of the hydrophone.

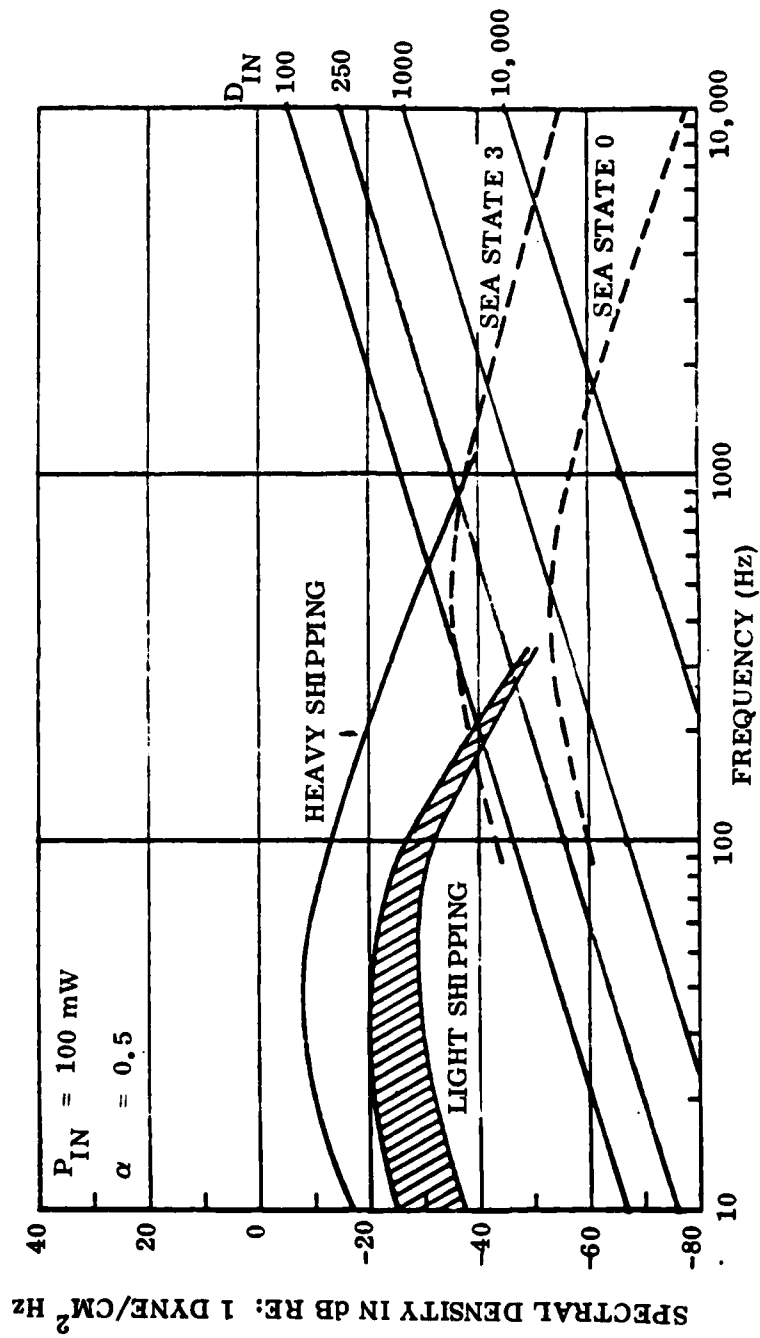


Figure 2-3. Optical Grating Hydrophone MDS Levels Superimposed on Background Sea Noise Curves

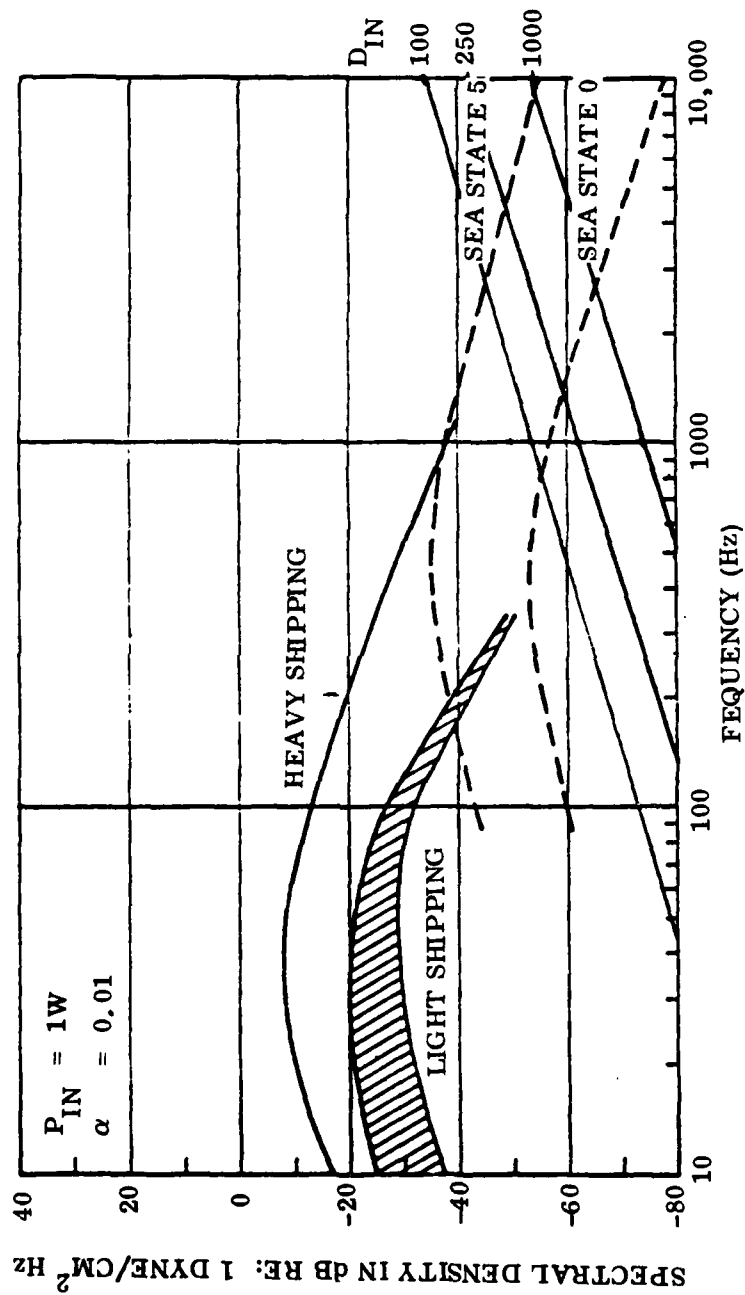


Figure 2-4. Optical Grating Hydrophone MDS Levels Superimposed on Background Sea Noise Curves

SECTION III

CONCLUSIONS AND DISCUSSION ON THE OPTICAL GRATING HYDROPHONE

The optical grating hydrophone is one of the most promising intensity modulating acoustic sensing device of those presently being considered [2] . Several models of the optical grating hydrophone have been built, of both the pressure sensing and pressure gradient sensing types [7] [12] . These models have displayed sensitivities close to predicted values.

As an intensity modulating device, the optical grating hydrophone offers the advantages associated with these types of optical sensors:

1. The output is a direct intensity modulated representation of an incident acoustic field, hence only a simple photodiode is required for detection.
2. Compatibility with other optical processing devices requiring intensity modulated inputs.
3. Either coherent or noncoherent light may be used. The light source may, therefore, be an inexpensive incandescent bulb.
4. Large, multimode optical conductors may be used to deliver high optical intensities to the device and photodetector. Larger fibers or optical conductors are much easier to handle from a mechanical point-of-view than are the significantly smaller single-mode fibers required by phase-modulating techniques.
5. The intensity devices are, in general, photon-noise limited, hence arbitrarily high sensitivities can be achieved by increasing the optical power.

In addition to these, the optical grating technique offers additional advantages over other intensity modulating methods:

1. The optical grating approach is relatively easy to conceptualize and analyze.
2. The gratings and their static setting allows much design flexibility with regards to hydrophone sensitivity and dynamic range.
3. The optical grating hydrophone can be fabricated rather easily and involves only state-of-the-art optical techniques.

The optical grating hydrophone has its drawbacks, especially when attempting to achieve high sensitivities such as sea-state zero noise detection above 1000 Hz. Primarily, high sensitivities require higher grating densities (for fixed values of optical power).

High density gratings (> 2500 lines/in.) begin to require tighter mechanical tolerances to maintain grating alignment, close spacing between the gratings, and proper bias (static) displacements. In addition, diffraction effects become more pronounced and will tend to decrease hydrophone performance.

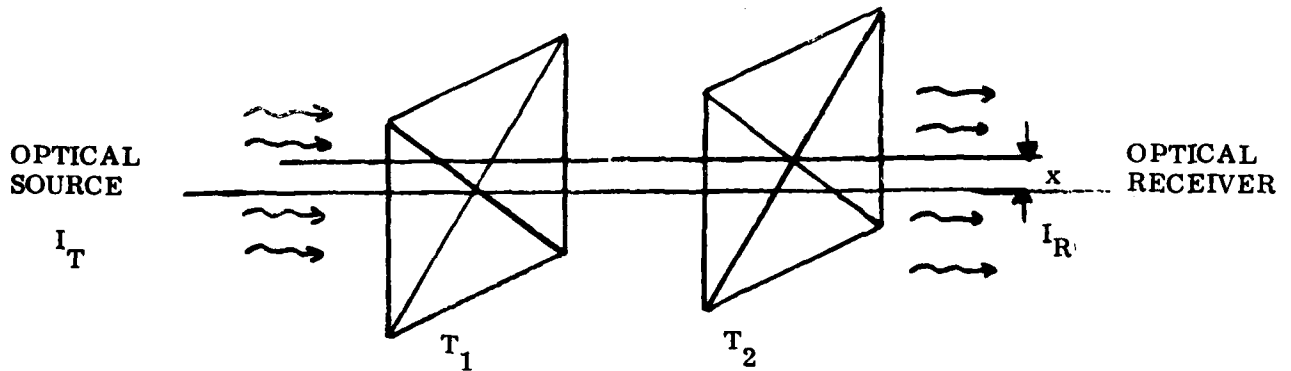
It is beyond the scope of this report to derive quantitative effects of misalignment, spacing, and diffraction on the performance of the optical grating hydrophone. An effort is currently in progress to do so, and will be the subject of a subsequent report. At this point, suffice it to say that the hydrophone performance analysis described herein assumes that Equation 4-7 is adequately approximated by the optical components of the hydrophone.

SECTION IV

ANALYSIS

4.1 THEORETICAL INTRODUCTION

Given two optical apertures which lie between an optical source and optical receiver, let T_1 be the optical transmittance function to the first optical aperture, and T_2 be the optical transmittance function of the second optical aperture. Let x denote the relative displacement of the two optical apertures as shown in the sketch below:



Ideally, neglecting diffraction effects, the overall transmittance function T is the correlation of the individual transmittance function T_1 and T_2 over the region common to both optical apertures:

$$T(x) = \int_{CA} T_1(\delta) T_2(x + \delta) d\delta \quad ; \quad CA = \text{Common Area of } T_1 \text{ and } T_2 \quad . \quad (4-1)$$

For the case in which T_1 or T_2 or both are symmetric about $X = 0$, then T is the convolution of T_1 and T_2 ,

$$T(x) = \int_{CA} T_1(\delta) T_2(x - \delta) d\delta \quad . \quad (4-2)$$

For this case, the following spatial fourier transform relation can be written:

$$\mathcal{F}\{T(x)\} = \mathcal{F}\{T_1(x)\} \mathcal{F}\{T_2(x)\} \quad (4-3)$$

where $\mathcal{T}\{T\}$ is the spatial Fourier transform of T , etc.. Hence, the transmittance function T can be found by taking the inverse transform of the product of the Fourier transforms of the individual transmittance functions.

For a light source of constant intensity, I_T , the received intensity, I_R can be written as:

$$I_R = I_T T(X) \quad (4-4)$$

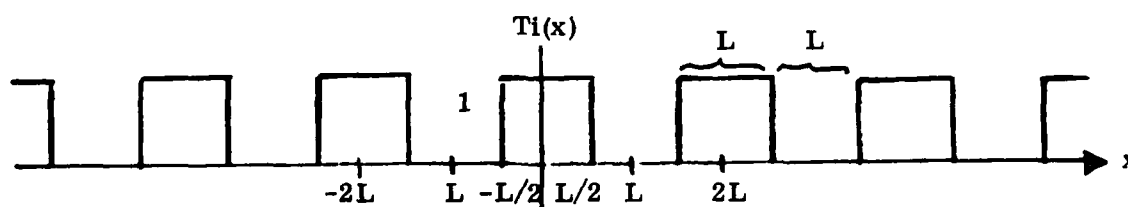
or, in normalized form:

$$I_R/I_T = T(X) \quad (4-5)$$

So, the received light intensity is a function of $T(X)$, the overall transmittance of the optical apertures.

To obtain a linear relationship between the overall transmittance T , and the displacement x , rectangular gratings can be used whose line widths and spacings are equal.

Such a transmittance function is sketched below:

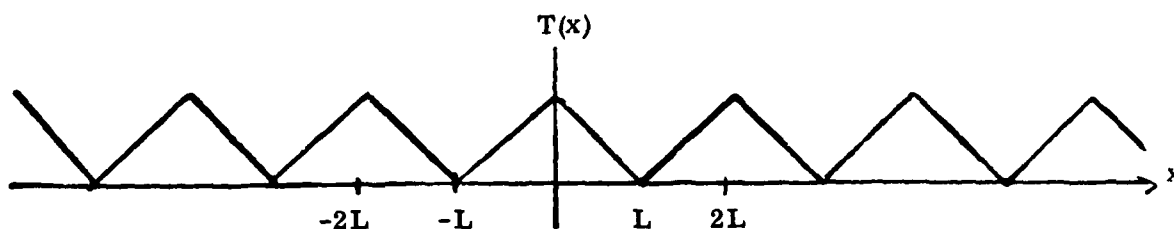


where L is the line (or space) width of the rectangular grating.

This can be expressed in Woodward's notation as:

$$T_1 = T_1 = T_2 = \text{REP}_{2L} [\text{RECT } x/L] \quad (4-6)$$

The overall transmittance T is simply the convolution of the two transmittance functions T_1 and T_2 , or, since $T_1 = T_2$, then T is simply the autocorrelation of T_1 , and is sketched below:



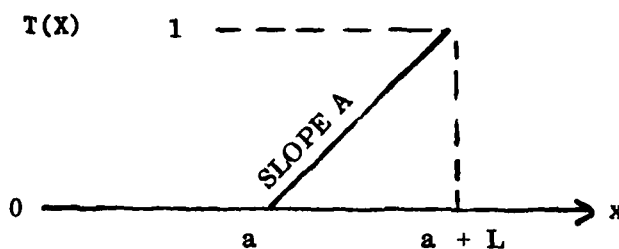
or

$$T(X) = \text{REP}_{2L} [\text{TRIANG } x/L] \quad (4-7)$$

The gain of the system is given by the slope of the transmittance function $T(X)$, or in other words, if A is the gain, then:

$$A = \Delta T(X) / \Delta X$$

Assume that the system ideally operates over only a portion of $T(X)$, where $a \leq x \leq a + L$ as shown below:



In this region, $T(x)$ can be represented by a gain factor times x_a :

$$T(x) = A x_a, \text{ where } x_a \text{ is referenced to } a,$$

or,

$$T(x) = A (x-a)$$

The range of $T(x)$ is 0 to 1. To achieve this, x , the total relative grating displacement must be L , since:

$$T(x) \Big|_{x=a} = 0 \quad (4-8)$$

and

$$T(x) \Big|_{x=a+L} = AL = 1 \quad (4-9)$$

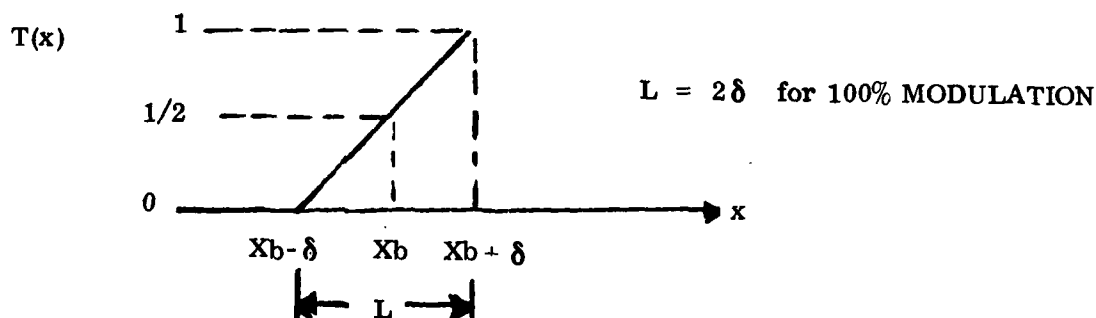
Hence, the system gain, A , can be written as:

$$A = 1/L \quad (4-10)$$

over the given range of $T(x)$.

The gain then is inversely proportional to the grid spacing, L , hence, the finer the grating, the higher the gain. In fact, virtually any given displacement x can be made to adequately modulate the optical bias level by properly choosing L .

For example, if the bias level was $T(x) = 1/2$, then spatial displacements $x = \pm \delta$ about the bias point will modulate the signal 100% if L is chosen such that $L = 2\delta$. $T(x)$ will therefore cover its entire range of 0 to 1 resulting in 100% modulation as sketched below:



The optical bias level can be calculated by summing $T(x_b)$ over that area exposed by the optical source.

Assume that a rectangular grating of dimension $H \times W$, where H is the total height, and W is the width of each grating, is uniformly illuminated by an optical source of total intensity I_T shown in Figure 4-1. Also assume that the bias point is at $X_b = \alpha L$, where α is a measure of the bias. For $\alpha = 0$, no light is transmitted, and for $\alpha = 1$, half of the available light is transmitted.

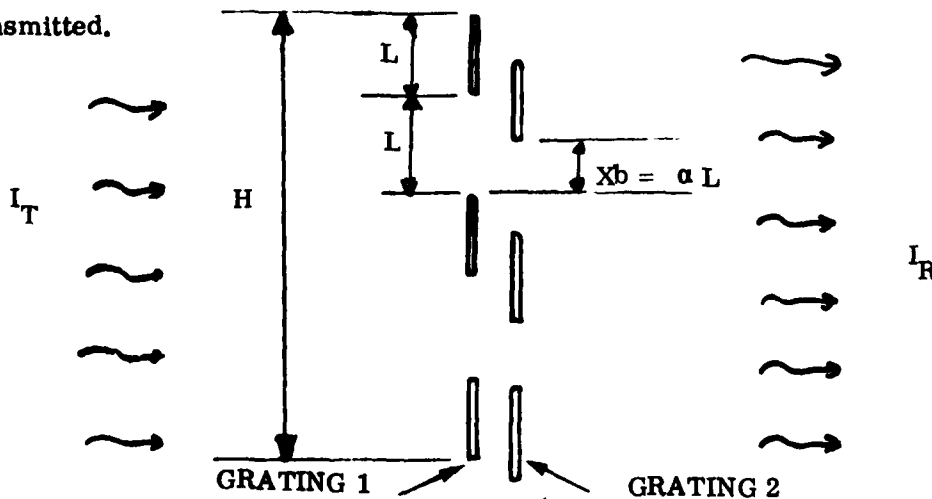


Figure 4-1. Rectangular Grating (Dimension HW) Uniformly Illuminated by Total Intensity Optical Source

Letting N = number of illuminated spaces

A_T = Total area of spaces

α = Constant, such that $0 \leq \alpha \leq 1$

Then the following relationships can be written:

$$(2N + 1) L = H \quad (4-11)$$

so the total number of spaces can be written:

$$N = \frac{H-L}{2L} \quad (4-12)$$

or conversely, L can be written as a function of N as:

$$L = \frac{H}{2N+1} \quad (4-13)$$

The total area of the spaces can then be written as:

$$A_T = NLW\alpha \quad (4-14)$$

or, in terms of N

$$A_T = \frac{NHW\alpha}{(2N+1)} \quad (4-15)$$

In terms of L ,

$$A_T = \frac{(H-L)W\alpha}{2} \quad (4-16)$$

But HW is the total available area, which corresponds to the maximum light intensity available, I_T . The received light intensity I_R can then be expressed as:

$$I_R = I_T A_T = I_T \left(\frac{N\alpha}{2N+1} \right) = I_T \frac{H-L}{2H} \alpha \quad (4-17)$$

or

$$\frac{I_R}{I_T} = T(x_b) = \frac{N\alpha}{(2N+1)} = \frac{(H-L)\alpha}{2H} \quad (4-18)$$

For the case of high desired gains, L is small and N is large, so:

$$\lim_{L \rightarrow 0} \frac{I_R}{I_T} = \lim_{L \rightarrow 0} T(x_b) = \lim_{N \rightarrow \infty} T(x_b) = \frac{\alpha}{2} \quad (4-19)$$

Therefore, despite the grid density, approximately $\alpha/2$ of the total optical source intensity is available at the output.

The movable grating technique has been demonstrated to be an effective acoustic detector in the laboratory. The optical source, receiver, and grating geometry for design implementations must adequately approximate Equation (4-7).

4.2 PERFORMANCE ANALYSIS

The performance of the optical grating hydrophone depends on the ability to detect the modulation of a light beam, the detection performed in the presence of system noise (electronic and photon), and the modulation produced by acoustic-pressure-induced motion of a grating. The noise mechanisms are analyzed, photon noise is shown to be dominant, and detectable light levels are shown to be readily realized in the presence of this dominant noise. Hydrophone sensitivity and dynamic range are then analyzed and shown to be of practical utility. Only state-of-the-art technology was assumed in the analyses.

4.2.1 SYSTEM NOISE

The ability to detect small displacements of the grating from a rest bias point in the optical hydrophone is ultimately limited by noise in the output of the optical detector. There are four important noise sources to consider:

1. Electronic
2. Thermal
3. Photon
4. Homodyne

4.2.2 ELECTRONIC NOISE

Electronic noise, in this case the detector noise, is the noise attributable to nonoptical origins. Typically these noise sources are shot noise, excess noise, and thermal noise. Shot noise is produced by the reverse bias current in the device. At low frequencies the shot noise increases with a $1/f$ characteristic and is referred to as excess noise. Thermal noise is produced by the series resistance, load resistance, and channel resistance of the device.

A noise power figure-of-merit for a photodetector is the noise equivalent power (NEP). This defines the minimum incident power required to generate a photocurrent equal to the total photodetector noise current. The formula for NEP is:

$$\text{NEP} = \frac{\text{Noise Current (A)}}{\text{Sensitivity (A/W)}} \quad (4-20)$$

Typically, the NEP is specified in terms of source wavelength, frequency of measurement, and noise bandwidth.

A typical photodiode, for example EG&G's HAD-1020A photodiode/operational amplifier, when configured to operate linearly to 10 kHz, has a NEP, at $\lambda = 0.9$ and $f = 10$ Hz, of about 10^{-12} W/ $\sqrt{\text{Hz}}$. The NEP over a 10-kHz band is less than 10^{-10} W.

This implies that, in the frequency range from 10 Hz to 10 kHz, optical powers above 10^{-10} W will dominate over detector noise. Realistic light levels are well above this noise floor, so detector noise is not expected to significantly affect performance.

4.2.3 RESISTOR THERMAL NOISE

For a detector operated in the photoconductive mode, the bias resistor used will generate a voltage that is a result of the thermal noise of the resistor.

The voltage induced by the thermal noise is given as:

$$V_T^2 = 4KTBR \quad (4-21)$$

where:

V_T = Voltage noise

K = Boltzmann's constant (1.38×10^{-23} J/ $^{\circ}\text{K}$)

T = Temperature in $^{\circ}\text{K}$

B = Bandwidth of measurement

R = Resistance of resistor

For a resistance value of 33.2K Ω at room temperature, 70 $^{\circ}\text{F}$ or 294 $^{\circ}\text{K}$, the noise voltage is:

$$V_T^2 = -153 \text{ dBv/Hz} \quad (4-22)$$

4.2.4 PHOTON NOISE

As light levels increase well beyond limits imposed by the thermal or electrical noise, photon noise associated with the average bias light dominates. Photon noise is physically the result of the random emission times of the discrete conduction electrons. These random emission times result in a fluctuation in the average current (i.e., noise). The noise is spectrally white because of the impulse nature of the current increment contributed by each electron. The signal-power to photon-noise-power ratio increases linearly with the increasing optical power that illuminates the photodetector.

The mean squared value of the current fluctuation due to shot noise (photon noise) in a photodetector is:

$$i_{np}^2 = 2eBi = \frac{V_{np}^2}{R^2} \quad (4-23)$$

where:

i_{np}^2 = Mean squared photon noise current in photodetector

V_{np}^2 = Mean squared photon noise voltage in photodetector

i = Direct current in photodetector

V = Bandwidth over which i_{np} is measured

e = Charge of electron = 1.6×10^{-19} C

R = Bias resistor in detector circuit

The current at which photon noise equals thermal noise (i_{EQ}) occurs when:

$$V_{np}^2 = V_T^2 \quad (4-24)$$

From the previous two equations for V_{np}^2 and V_T^2 , this relationship becomes:

$$2eBi_{EQ}R^2 = 4KTBR \quad (4-25)$$

Solving for i_{EQ} yields:

$$i_{EQ} = \frac{2KT}{eR} \quad (4-26)$$

For typical values $T = 294^\circ$ and $R = 33,200 \Omega$, i_{EQ} becomes:

$$i_{EQ} \approx 1.5 \times 10^{-6} \text{ A}$$

For photodetectors with quantum efficiencies of 50%, this corresponds to an optical power of $3 \mu\text{W}$.

Optical intensities considerably above this are common in optical fibers, so photon noise will generally dominate over thermal noise.

4.2.5 HOMODYNING NOISE (by Joe Chovan)

The reduction in noise with increasing optical power continues up to a limit where homodyning noise becomes dominant. Homodyning noise occurs with any optical source that has a finite spectral (color) width. Physically, it is due to different optical frequency components in the electronic signal out of the photodetector mixing together. As the optical power is increased, homodyning noise increases at the same rate as the signal so that no further signal-to-noise improvement is realized.

A photodetector is a power detector, responding to the square of the input optical time waveform. Multiplying a time function by itself is equivalent to convolving the complex spectrum with itself in the frequency domain. The time waveform out of an incoherent light source can be considered as a random variable with a Gaussian amplitude probability distribution. Thus, the frequency spectrum out of the photodetector is the convolution of the power spectrum of the light source with itself [13] .

For simplicity, consider the optical power spectrum out of the optical source to be rectangular with a bandwidth β as shown in Figure 4-2. The power spectrum out of the detector is then an impulse at dc and a triangular spectrum extending to 2β as shown. This component is of no interest since the photodiode detector current can not respond at this frequency.

In actual practice, the input spectrum is typically more Gaussian-shaped than rectangular, so the output spectrum is also Gaussian-shaped with twice the spread. In either case, the input spectrum is so broad that the output region of interest is confined near dc, comparatively speaking. Thus, the spectrum can be considered as essentially flat over the region of interest.

The important point is that the power spectral density of the output current noise equals the squared dc current divided by the optical bandwidth as shown in Figure 4-2. Physically, this noise is due to the incoherent power summation of the various difference frequencies within the optical spectrum mixing in the photodetector. The dc component, on the other hand, arises from the coherent mixing of each spectral component with itself.

Optical bandwidth is determined from the spectral line width of the source as follows:

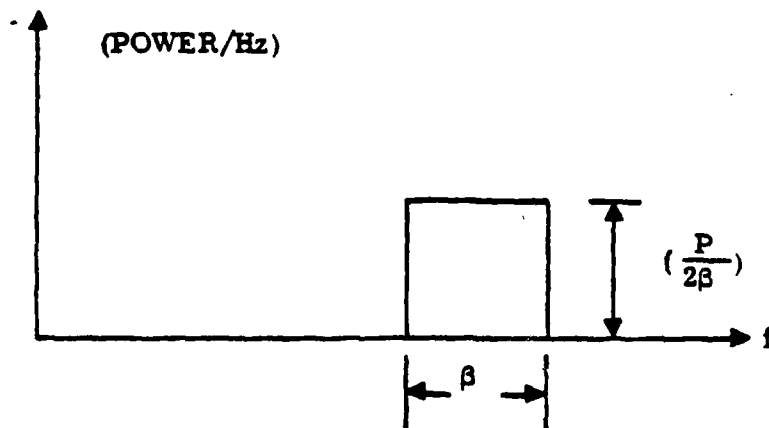
$$B = \frac{\Delta \lambda c}{\lambda^2} \quad (4-27)$$

where:

- B = Frequency bandwidth of optical spectrum out of optical source
- λ = Nominal optical wavelength of optical source
- $\Delta \lambda$ = Nominal spread of wavelength in output spectrum of optical source
- c = Speed of light = 3×10^8 m/s

OPTICAL SPECTRAL
DENSITY INTO PHOTODETECTOR

P = TOTAL OPTICAL POWER INTO
PHOTODETECTOR



OPTICAL SPECTRAL
DENSITY OF PHOTODETECTOR
OUTPUT

I_{dc} = dc CURRENT OUT OF
PHOTODETECTOR

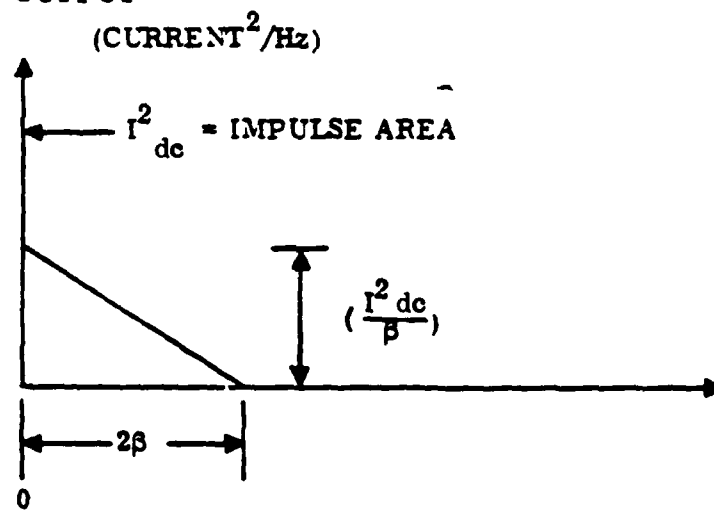


Figure 4-2. Optical Power Spectrum

With such a flat noise approximation, the mean-squared homodyne noise current in a bandwidth B is:

$$i_{nh}^2 = \frac{i^2}{\beta} B \quad (4-28)$$

where:

i_{nh}^2 = Mean-squared homodyne noise current in photodetector

β = Optical bandwidth

i = Direct current in photodetector

B = Bandwidth over which i_{nh} is measured.

This homodyne noise analysis appears plausible when applied to a local area on the photodetector surface that is small enough for the optical wavefronts to be well correlated over the immediate neighborhood. However, when integrating over the entire surface of the photodetector, it is reasonable to expect that the homodyne noise is likely to be independent for regions that are separated enough that the optical wavefronts are no longer correlated. For such uncorrelated areas, the homodyne noise will add in power. This noise is basically a fluctuation in the detector current. On the other hand, the detector current will add directly for different areas on the photodetector surface (i.e., for uniform optical power per unit area, the average detector current can be expected to double by doubling the area, while the RMS fluctuations in the detector current will only increase by a factor of $\sqrt{2}$).

This integration gain realized by averaging over a large number of independent regions on the photodetector surface is expected to be very significant.

As an example, consider an optical fiber having a 400 micron core diameter and a numerical aperture of 0.2. Such fibers are commercially available with low attenuation and are representative candidates for use with the optical grating hydrophone.

The numerical aperture dictates the region on the fiber face over which the optical wavefronts behave monotonically and are well correlated. As a nominal rule of thumb, the diffraction angle associated with this correlation area (i.e., the average optical wavelength divided by the diameter of the correlation area) can be taken as equal to the angle dictated by the numerical aperture of the fiber. Using a nominal

optical wavelength of 0.6 microns and a numerical aperture of 0.2 implies a correlation diameter of about 3 microns.

Dividing the total area of the 400 micron fiber core by the area of the 3 micron correlation neighborhood indicates about 1.8×10^4 independent subareas on the fiber face to be summed.

Thus, the squared homodyne noise current will be

$$i_{nh}^2 = \frac{i_e^2 B}{\beta (1.8 \times 10^4)}$$

Comparing this homodyne noise current with the photon noise current given previously, it is seen that homodyne noise dominates for large i and photon noise dominates for small i .

The current for which these two noises are equal is determined as follows:

$$\text{For } i_{np}^2 = i_{nh}^2 \quad (4-29)$$

$$2eBi_e = i_e^2 \frac{B}{\beta (1.8 \times 10^4)} \quad (4-30)$$

$$i_e = 2e\beta (1.8 \times 10^4) \quad (4-31)$$

where:

i_e = Photodetector dc current for which homodyne noise equals photon noise.

The optical power corresponding to this detector current is determined as follows:

The optical power (P) divided by the energy per photon ($h c / \lambda$) yields the number of photons multiplied by the quantum efficiency (η), which yields the number of conduction electrons per second. This number of conduction electrons per second multiplied by the charge of an electron (e) yields the detector current.

$$i = \frac{P \lambda \eta e}{h c} \quad (4-32)$$

where:

- P = Optical power illuminating photodetector
- λ = Optical wavelength (nominal)
- η = Quantum efficiency of photodetector
- h = Plank's constant = 6.625×10^{-34} Ws²
- c = Speed of light = 3×10^8 meter/m/s
- e = Electron charge = 1.6×10^{-19} W.

The optical power for which photon noise equals homodyne noise is determined from the previous two equations as follows:

$$(1.8 \times 10^4) 2e\beta = i_e = \frac{P_e \lambda e \eta}{h c} \quad (4-33)$$

$$P_e = \frac{2 h c \beta (1.8 \times 10^4)}{\lambda \eta} \quad (4-34)$$

where:

P_e = optical power for which homodyne noise equals photon noise.

For low-loss multimode optical fiber having $\lambda = 1.05 \mu$ and $\beta = 2.14 \times 10^{14}$ Hz, the above equation yields

$$P_e = 1.46 \text{ W.} \quad (4-35)$$

Photodetectors having quantum efficiencies exceeding 50% are readily available. Thus, optical powers exceeding about 3 W onto the photodetector can be expected to be homodyne-noise-limited. No further SNR improvement is realized for higher optical powers.

4.2.6 CONCLUSION ON OPTICAL NOISE

Since optical powers of less than 1W into an optical fiber are common, homodyne noise will not be a factor. Using larger fibers will increase the homodyne noise limit even further if necessary.

Thus photon noise, rather than homodyne noise, will continue to be the dominant noise source for any optical power levels of practical interest in the optical grating hydrophone system.

This is confirmed by the experimental data presented in Appendix A. The data indicates that photon noise rather than homodyne noise remained as the limiting factor over the entire range experimentally investigated.

Notice that at the higher light levels, SNR's as high as 160 dB were experimentally realized. This corresponds to a minimum detectable grating displacement of 10^{-8} cycles. Thus, grating as coarse as 10 cycles/mm can be used to sense displacements as small as 0.01 Å. In view of these figures, acoustic sensitivity is not expected to be a problem.

4.3 SENSITIVITY/DYNAMIC RANGE ANALYSIS

4.3.1 GENERAL

Assuming that photon noise is now the dominant factor, sensitivity calculations can be made.

The photon noise is given by: (4-36)

$$i_p^2 = 2ei_T B$$

where

$$i_p^2 = \text{Photon noise current}$$

$$e = \text{Electron charge}$$

$$i_T = \text{Total average current}$$

$$B = \text{Bandwidth of measurement.}$$

For a given signal current, i_s , the signal-to-photon-noise ratio becomes:

$$SNR_p = \frac{i_s^2}{2ei_TB} \quad (4-37)$$

Relating current to optical power we can write:

$$i_s = \frac{P_s \eta e}{h\nu} \quad (4-38)$$

$$i_T = \frac{P_T \eta e}{h\nu} \quad (4-39)$$

where

- P_s = Optical signal power
- P_T = Optical bias, or average power
- h = Planck's constant
- ν = Optical frequency
- η = Quantum efficiency

The signal-to-photon-noise ratio can now be expressed as:

$$SNR_p = \left(\frac{P_s \eta e}{h\nu} \right)^2 \frac{hf}{P_T \eta e} \frac{1}{2eB} \quad (4-40)$$

$$= \frac{P_s^2}{P_T} \frac{\eta e}{h\nu} \frac{1}{2eB} \quad (4-41)$$

$$= \frac{P_s^2}{P_T} \frac{\eta}{2h\nu B} \quad (4-42)$$

The optical power through the gratings, assuming a bias of X_o , can be written as:

$$P_T = P_o + P_s = \frac{[X_o + \delta(t)] P_{in}}{2L} \quad (4-43)$$

where

- X_o = Bias position
- L = Distance between grating lines
- $\delta(t)$ = Small distance variation due to signal
- P_{in} = Input optical power to hydrophone
- P_o = Optical bias power through hydrophone
- P_s = Optical signal power through hydrophone

P_o and P_s can be written as:

$$P_o = \frac{X_o P_{in}}{2L} \quad (4-44)$$

$$P_s = \frac{\delta(t) P_{in}}{2L} \quad (4-45)$$

Plugging P_s and P_o into the expression for SNR_p results in:

$$SNR_p = \frac{\delta^2(t) P_{in}^2 \eta}{4L^2 2h\nu B} \frac{2L}{[X_o + \delta(t)] P_{in}} \quad (4-46)$$

$$= \frac{\delta^2(t) P_{in} \eta}{4L h\nu B (X_o + \delta(t))} \quad (4-47)$$

For $\delta(t) \ll X_o$ this equation reduces to:

$$SNR_p = \frac{\eta P_{in}}{4h\nu B} \frac{\delta^2(t)}{L X_o} \quad (4-48)$$

Now let us assume that the bias point X_o is some fraction of L :

$$X_o = aL \quad (4-49)$$

Then SNR_p becomes:

$$SNR_p = \frac{P_{in} \eta}{4h\nu B} \frac{\delta^2(t)}{aL^2} \quad (4-50)$$

At $\delta = \alpha L$, SNR_p becomes maximum

$$SNR_{pmax} = \frac{P_{in} \eta \alpha}{8 h \nu B} = \text{dynamic range} \quad \text{(Referenced to 0 dB } SNR_p) \quad (4-51)$$

To determine the minimum displacement that could be detected $\delta_m^2(t)$, let $SNR_p = 1$ such that signal power is just equal to the photon noise power. Solving for $\delta_m^2(t)$ yields:

$$\delta_m^2(t) = \frac{4 h \nu B \alpha L^2}{P_{in} \eta} \quad (4-52)$$

We relate this to particle motion in water due to a sound pressure level P :

$$d = \frac{P}{\omega \rho c} \quad (4-53)$$

where

d = Particle motion in water

ω = Acoustic frequency

ρc = Acoustic impedance

The actual relationship between the displacement and the acoustic power in the water depends on the vibrating sensing diaphragm that drives the grating shutter. Here, an upper bound is assumed on this displacement for nonresonant structures by considering that the diaphragm cannot move through excursions that exceed those of free water particles in the acoustic field.

Solving for P^2/B results in:

$$\frac{P^2}{B} = \frac{4 h \nu (\omega \rho c)^2 \alpha L^2}{P_{in} \eta} \quad (4-54)$$

which gives the minimum sound pressure level in a bandwidth B that results in an optical signal-to-photon-noise ratio at the hydrophone output of 0 dB. In other words this is the calculated minimum detectable sound pressure level of the intensity grating hydrophone (MDS level), or detection Threshold Level.

Relating this to the spatial frequency of the optical gratings, D , where

$$D = \frac{1}{2L} \quad (4-55)$$

we can write:

$$\frac{P^2}{B} = \frac{h \nu (\omega \rho c)^2 a}{P_{in} \eta D^2} = \frac{h \nu (\omega \rho c)^2}{\eta} \cdot \frac{a}{P_{in} D^2} \quad (4-56)$$

or by letting $\omega = 2\pi f$

$$\frac{P^2}{B} = \frac{h \nu (2\pi \rho c)^2}{\eta} \frac{f^2 a}{P_{in} D^2} \quad (4-57)$$

where

$$h = 6.63 \times 10^{-34} \text{ J-s}$$

$$\nu = 4.5 \times 10^{14} \text{ Hz}$$

$$\eta = 0.5$$

$$\rho c = 1.55 \times 10^5 \text{ gm cm}^{-2} \text{ s}^{-1}$$

which results in:

$$\frac{P^2}{B} = (3.651 \times 10^{-6}) \frac{f^2 a}{P_{in} D_i^2} \quad (4-58)$$

with D_i in units of lines per inch and P_{in} in units of watts .

This equation implies that the system sensitivity can be increased (MDS level decreased) by either:

- Increasing grating densities, D_i
- Increasing optical power, P_{in}
- Decreasing the bias, a
(at the expense of dynamic range)

4.3.2 MINIMUM BIAS (a)

Theoretically, a can be adjusted such that the optical throughput results in

photon noise equal to detector noise. Beyond this point, sensitivity can no longer be increased.

To determine what value of a can be used, a_m , let us express the input and output optical power (P_{in} and P_o respectively) in terms of a :

$$P_o = \frac{a_m P_{in}}{2} \quad (4-59)$$

$$\text{so } a_m = 2P_o/P_{in} \quad (4-60)$$

We can also write:

$$\frac{P_o \eta e}{h\nu} = i_o \quad (4-61)$$

where i_o = photodiode current corresponding to P_o .

By letting i_o equal the current at which photon noise equals detector noise, i_D , which is a measurable quantity, the power corresponding to this noise can be expressed as:

$$P_o = \frac{i_D h\nu}{\eta e} \quad (4-62)$$

Plugging this into the expression for a_m yields:

$$a_m = \frac{2i_D}{P_{in}} \frac{h\nu}{\eta e} \quad (4-63)$$

This can be used in the MDS equation to give:

$$\frac{P^2}{B} = \frac{h\nu (2\pi\rho c)^2}{\eta} \left(\frac{f^2 a_m}{P_{in} D^2} \right) \quad (4-64)$$

$$= \frac{h\nu (2\pi \rho c)^2}{\eta} \left(\frac{f^2}{P_{in} D^2} \right) \left(\frac{h\nu}{\eta e} \right) \frac{2i_D}{P_{in}} \quad (4-65)$$

$$= 2 \left(\frac{h\nu}{\eta} \right)^2 \frac{(2\pi \rho c)^2}{e} \left(\frac{f^2 i_D}{P_{in}^2 D^2} \right) \quad (4-66)$$

Since it was assumed that in selecting α_m , the photon noise was equal to detector noise, the MDS expression should be multiplied by 2 which compensates for the 3 dB loss in actual SNR to give:

$$\frac{P^2}{B} = \left(\frac{h\nu}{\eta} \right)^2 \frac{(2\pi \rho c)^2}{e} \frac{i_D f^2}{P_{in}^2 D^2} \quad (4-67)$$

$$= \frac{i_D}{e} \left(\frac{h\nu}{\eta} \right)^2 \left(\frac{4\pi \rho c f}{P_{in} D} \right)^2 \quad (4-68)$$

$$= \frac{i_D}{e} \left(\frac{h\nu 4\pi \rho c f}{P_{in} D} \right)^2 \quad (4-69)$$

$$= (5.447 \times 10^{-5}) \frac{i_D f^2}{P_{in}^2 D_1^2} \quad (4-70)$$

where: D_1 is in units of lines per inch.

The value of i_D was calculated previously (see photon noise section) for a typical photodiode with a $33.2K \Omega$ resistor and found to be equal to 1.5×10^{-6} .

Plugging this into the MDS equation yields:

$$\frac{P^2}{B} = (8.171 \times 10^{-11}) \frac{f^2}{P_{in}^2 D_1^2} \quad (4-71)$$

This is plotted in Figure 4-3 for representative parameters .

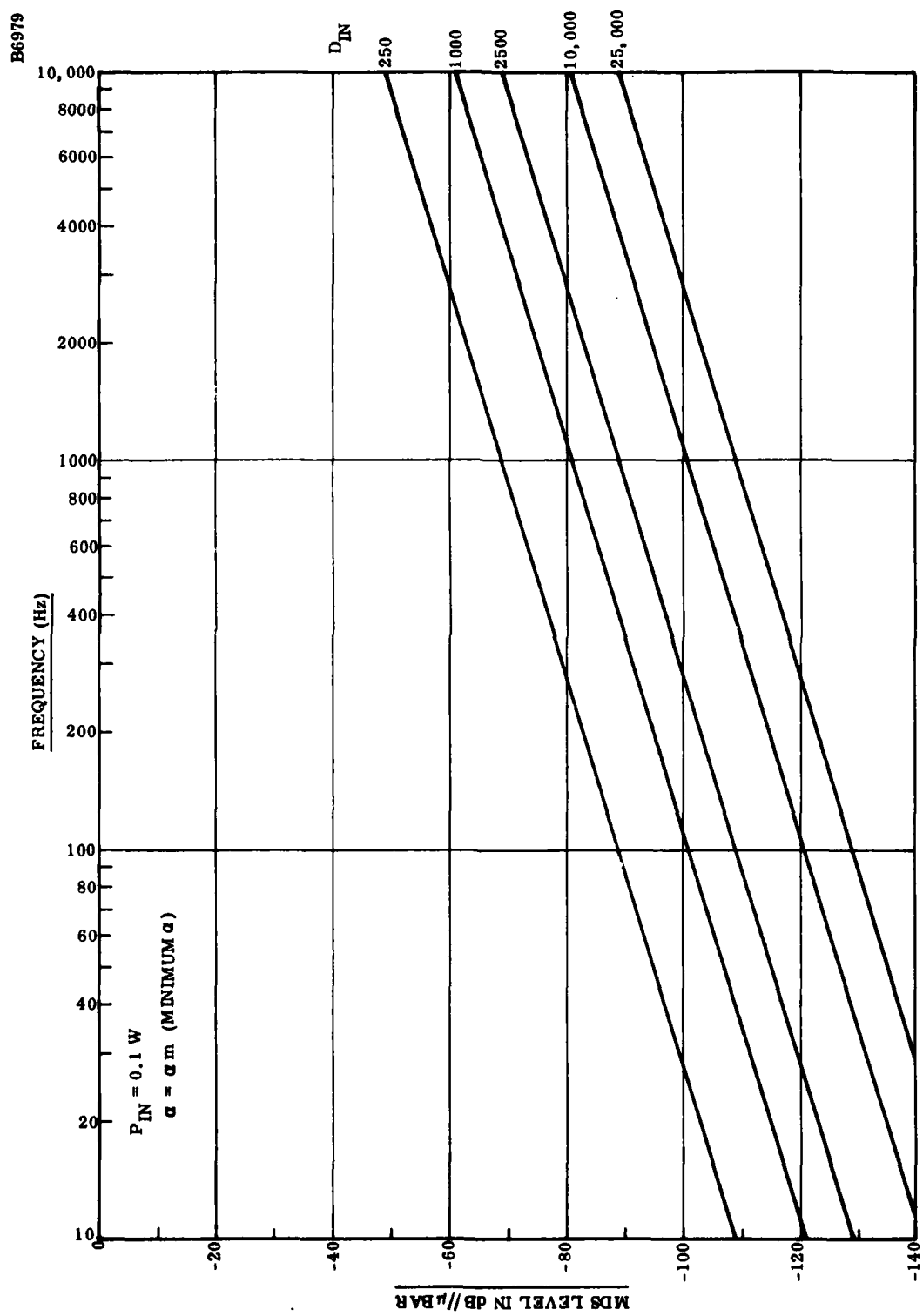


Figure 4-3. MDS Level vs. Frequency for $\alpha = \alpha_m$

The dynamic range can be expressed by plugging the expression for α_m into the equation for $\text{SNR}_p \text{ max}$ to give:

$$\text{DR} = \text{SNR}_p \text{ max} = \frac{P_{in} \eta_m}{8 h \nu B} = \frac{P_{in} \eta}{8 h \nu B} \cdot \frac{2 i_D h \nu}{P_{in} \eta e} = \frac{i_D}{4 e B} \quad (4-72)$$

For $i_D = 1.5 \times 10^{-6}$ Amps, the dynamic range is 126.7 dB.

SECTION V
REFERENCES

- [1] J.A. Bucaro, "Optical Hydrophones for Sonar", Naval Research Laboratory, Washington, D.C..
- [2] J. Bucaro and J.H. Cole "Acousto-Optic Sensor Development", Naval Research Laboratory, Washington, D.C..
- [3] P. Shajenko, "Progress on Optical Hydrophones", U.S. Navy Journal of Underwater Acoustics, Vol 29, No. 2, April 1979.
- [4] A. Mark Young, Theodore A. Henriquez, Allan C. Tims, "Fiber Optic Hydrophone for use as an Underwater Electroacoustic Standard", U.S. Dept. of Navy Patent Application PAT - APPL - 940550.
- [5] P. Shajenko, J.P. Flatley, M.B. Moffeit, "On Fiber-Optic Hydrophone Sensitivity", J. Acoust. Soc. Am. Vol 64, No. 5, Nov. 1978.
- [6] G. Hetland, C.M. Davis, R.E. Einzig, "Optical Sonar System Concepts".
- [7] W.B. Spillmor, Jr. and D.H. McMahon, "Schlieren Multimode Fiber-Optic Hydrophone; Appl. Phys. Lett. Vol 37, No. 2, July 15, 1980.
- [8] I. Fromm, H. Uterberger, "Direct Modulation of Light by Sound", Information from the Research Laboratories of Siemens AG Munich W-Germany, CH1305-2/79/0000-0040 \$00.75 C 1979 IEEE.
- [9] R.H. Pahler, Jr., A.S. Roberts, Jr., "Design of a Fiber Optic Pressure Transducer", Transactions of the ASME, Feb. 1977.
- [10] M. Stimler, "Opto-Acoustic Hydrophone", U.S. Patent 3,903,496, Sept. 2, 1975.
- [11] J.L. Walker, "Voice Recording and Reproducing Device, "U.S. Patent 1,186,717, June 13, 1916.
- [12] J. Jackson, "On the Design of Optical Hydrophones", NADC Contract #N62269-79-C-037.
- [13] W. Devenport, Jr., and W. Root, "An Introduction to the Theory of Radom Signals and Noise", McGraw Hill, 1958, Section 12.2.

APPENDIX A
OPTICAL NOISE MEASUREMENTS
(by E. Valovage)

1. INTRODUCTION

A measurement of optical noise was made using a photodetector whose output voltage is proportional to the incident light power. The noise is defined as the RMS value of the fluctuations of this voltage for a constant incident light power. Defining the signal as the dc component of this output voltage, a signal-to-noise ratio (SNR) parameter can be obtained. This SNR represents a suitable measure of the dynamic range of the detector, indicating the minimum value of fluctuations which can be detected for a given dc or average value.

2. PROCEDURE

The experimental setup is shown in Figure A-1. Details and specifications on the components are given in Table A-1. The average light power on the detector, as indicated by the dc voltmeter, was varied both by changing the voltage on the light source and by moving the source and lens. Noise measurements were consistent regardless of the manner in which the light power was varied. The photodiode output was amplified by a low noise amplifier with 40 dB of gain. The power spectral density of the noise, both electrical and optical, is flat from less than 1 kHz to greater than 20 kHz. Thus, noise measurements were taken in a 100-Hz band centered at 2 kHz, and tabulated values are referred to a 1-Hz band.

The self-noise of the system is measured with the photodiode in darkness. For low light levels, this noise floor puts a maximum on the attainable SNR according to:

$$\text{SNR} \leq 20 \log \left(\frac{V_{\text{dc}}}{V_{\text{ne}}} \right) \text{ dB} \quad (\text{A-1})$$

with

V_{dc} = Dc component of the photodiode output

V_{ne} = Electrical noise measured with photodiode dark.

The primary source of V_{ne} is the thermal noise voltage generated by the resistor (in this case $R = 33.2K\Omega$) in accordance with the following equation:

$$V_{ne}^2 \approx V_T^2 = 4KTBR \quad (A-1a)$$

where $K = \text{Bolzman's constant } (1.38 \times 10^{-23} \text{ J/}^\circ\text{K})$

$T = \text{Temperature in } ^\circ\text{K}$

$B = \text{Bandwidth of measurement}$

$V_T = \text{Thermal noise voltage}$

$R = \text{Value of resistor}$

For $T = 294 ^\circ\text{K} \quad (70^\circ\text{F})$

$B = 1 \text{ Hz}$

$R = 33.2K\Omega$

V_{ne}^2 becomes:

$$V_{ne}^2 = -153 \text{ dBV/Hz}$$

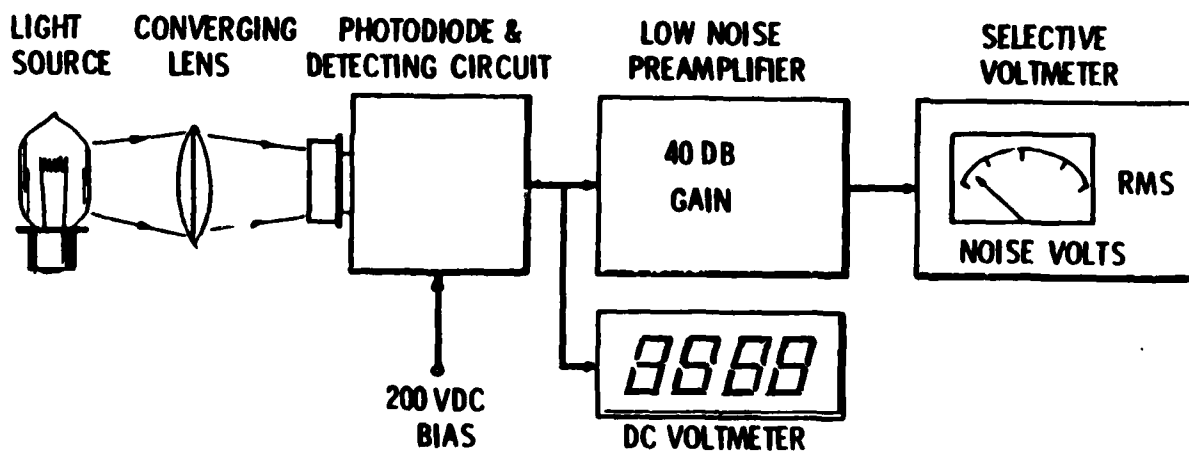
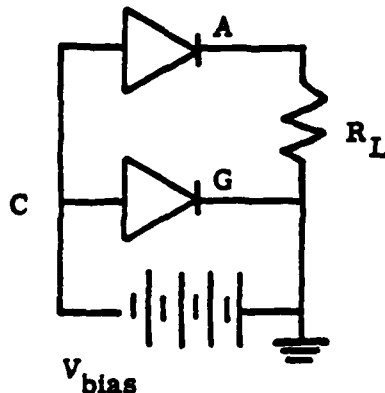


Figure A-1. The Optical Noise Measurement Test Setup

TABLE A-1
SPECIFICATIONS

Photodiode: EG &G SGD-040-A

"Silicon Diffused Guard Ring Diode"



Overall sensitivity
12.7 v/mW
in 400-1100 nm band

$R_L = 33.2 \text{ k}\Omega$

Light Source: 12V 55W "H3"

Quartz Halogen Bulb

(Fog and driving light applications)

Noise Measurement:

Hewlett Packard 3591A

Selective Voltmeter

Measurements taken in 100-Hz band at 2 kHz. Tabulations referred to 1-Hz band

Flatness of spectrum verified by HP 3580A Spectrum Analyzer

Dc Meter:

Fluke 8000A Digital Multimeter

Low Noise Preamp: 40-dB Gain

Self-Noise $-174 \frac{\text{dBV}}{\sqrt{\text{Hz}}}$

For higher light levels, where photon noise at the detector exceeds the electrical noise, the maximum SNR is limited by the photon noise, as given by:

$$\text{SNR} \leq 20 \log \left(\frac{V_{dc}}{V_{np}} \right) \text{ dB} \quad (\text{A-2})$$

with

$$V_{np} = \text{photon noise.}$$

The photon noise is dependent upon the average light power level and is given by:

$$V_{np}^2 = 2e V_{dc} RB \quad (\text{A-3})$$

with

$$e = \text{Electron charge } 1.6 \times 10^{-19} \text{ C}$$

$$R = \text{Load resistance in photodiode circuit}$$

$$B = \text{Bandwidth of measurement (1Hz).}$$

The above asymptotic limits (Equations A-1 and A-2) are plotted in Figure A-2. Since the noise voltages are RMS, their effects are combined near the crossover point yielding a SNR limit according to:

$$\text{SNR} \leq 10 \log \left(\frac{V_{dc}^2}{2e VR + V_{ne}^2} \right) \quad (\text{A-4})$$

This curve is plotted at the crossover of the asymptotes, representing the theoretical SNR value for various light levels.

Experimental data is tabulated in Table A-2. The system self-noise was measured with the photodiode dark. With a 200V bias on the photodiode, noise measurements were made for increasing light levels up to a reading of 56V on the dc voltmeter (35 dBV). The data points obtained are plotted on Figure A-2 along with the theoretical curve. The data is consistent with the theory to within one dB.

TABLE A-2
EXPERIMENTAL AND CALCULATED DATA

Dc Output		RMS Noise		SNR	
Volts	dBV	Calculated	Measured	Calculated	Measured
0.01	-40.0	152.2	151.5	112.2	111.5
0.03	-30.5	150.8	150.5	120.3	120.0
0.1	-20.0	148.0	148.0	128.0	128.0
0.3	-10.5	144.3	145.0	133.8	134.5
1.0	0	139.5	140.0	139.5	139.7
3.0	9.5	134.8	135.0	144.3	144.5
5.0	14.0	132.7	133.0	146.7	146.7
10.0	20.0	129.7	130.0	149.7	150.0
31.6	30.0	124.7	125.0	154.7	155.0
56.2	35.0	122.2	123.0	157.2	158.0

3. CONCLUSION

Assuming there are no noise sources other than detector noise and photon noise, the dynamic range (SNR) can be increased arbitrarily given enough average light power. If any other sources of noise exist such as to further limit theoretical SNR values, their effect is not seen here up to SNR values of 158 dB. Thus such limits, if any, must be well above 170 dB.

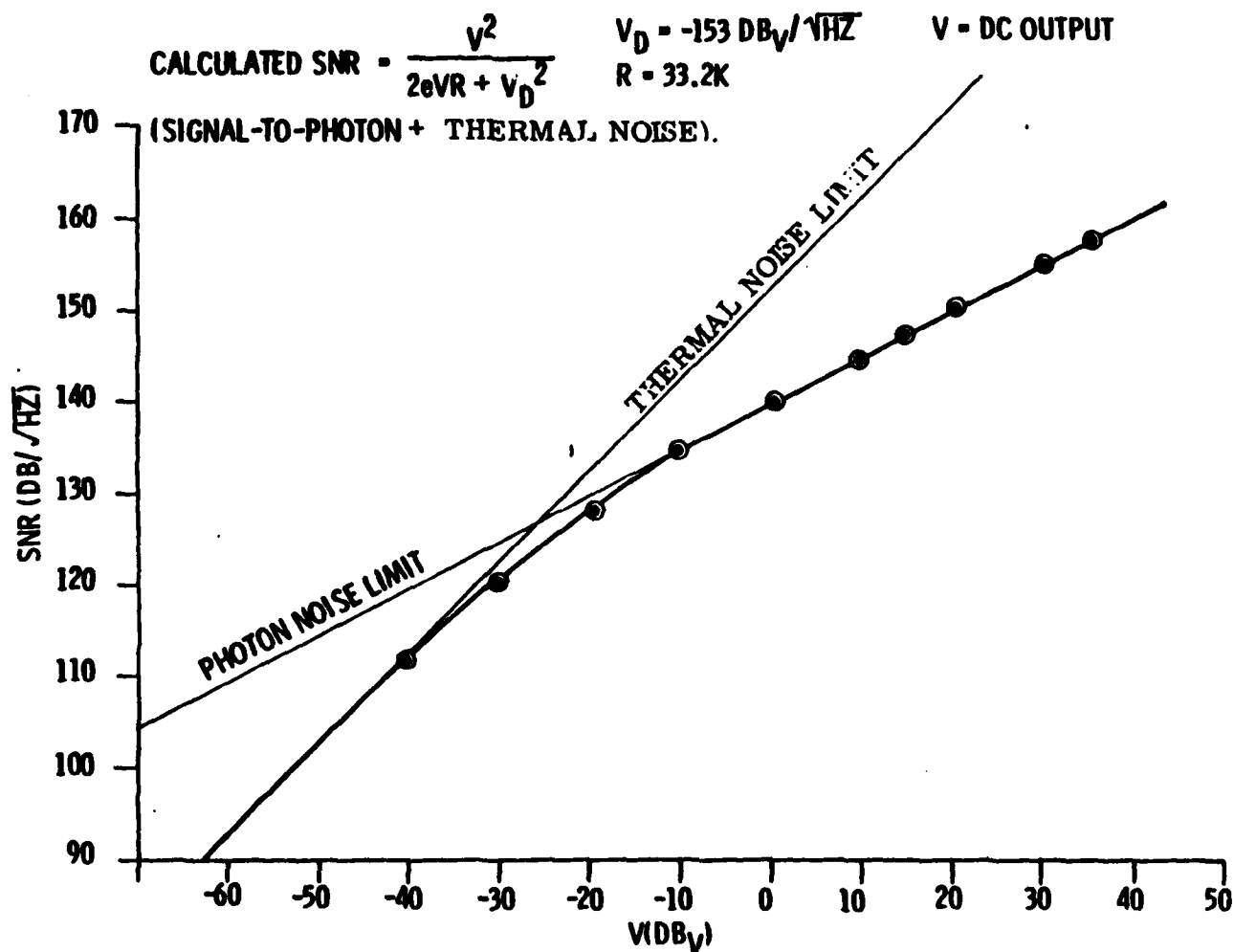


Figure A-2. Experimental and Calculated Data

DATE
FILMED
-8